BIOCELL
2023 47(1): 195-204

Tech Science Press

check for updates

Schisandrin B exerts anticancer effects on human gastric cancer cells through ROS-mediated MAPK, STAT3, and NF-κB pathways

Tianzhu LI[1,#]; Yu ZHANG[2,#]; Tong ZHANG[2,#]; Yannan LI[2]; Hui XUE[2]; Jinglong CAO[2]; Wenshuang HOU[2]; Yinghua LUO[3,*]; Chenghao JIN[2,4,*]

[1] Department of Molecular Biology, College of Basic Medical Science, Chifeng University, Chifeng, 024000, China
[2] Department of Biochemistry and Molecular Biology, College of Life Science and Technology, Heilongjiang Bayi Agricultural University, Daqing, 163319, China
[3] Department of Grass Science, College of Animal Science and Veterinary Medicine, Heilongjiang Bayi Agricultural University, Daqing, 163319, China
[4] National Coarse Cereals Engineering Research Center, Daqing, 163319, China

Key words: Schisandrin B, Gastric cancer, Reactive oxygen species, Apoptosis, Migration, Cell cycle

Abstract: Schisandrin B (Sch B) is a monomer with anti-cancer and anti-inflammatory effects, which are isolated from the plant *Schisandra chinensis* (Turcz) Baillon. We investigated the anti-gastric cancer (GC) effects of Sch B and its underlying molecular mechanisms. The Cell Counting Kit-8 assay was used to determine the effects of Sch B on the viability of GC and normal cell lines. Hoechst/propidium iodide staining and flow cytometry were used to assess the apoptosis induction of Sch B. Western blotting was used to evaluate the effects of Sch B on downstream apoptotic proteins. The DCFH-DA fluorescent probe was used to assess the regulatory effects of Sch B on reactive oxygen species (ROS) levels and related signaling pathways in GC cells. The results showed that Sch B could regulate the phosphorylation level of mitogen-activated protein kinase (MAPK) by upregulating ROS accumulation in gastric cancer cells, and then reduce the expression of nuclear factor kappa B (NF-κB) and phosphorylated transcription 3 (p-STAT3). In addition, Sch B downregulated the cell cycle proteins cyclin-dependent kinase 2/4/6 and cyclin D1/E, and arrested cells in the G0/G1 phase. Moreover, it also inhibited cell migration, which was reversed with N-acetylcysteine pretreatment. In summary, Sch B has killing effects on GC cells by upregulating the production of intracellular ROS and regulating the MAPK/STAT3/NF-κB signaling pathway, leading to the migration arrest and apoptosis of GC cells.

Introduction

Gastric cancer (GC) is one of the most common cancers and has the third highest cancer mortality rate (Rawla and Barsouk, 2019). Early symptoms of GC may not be noticeable, and many patients are already in the advanced stage when first diagnosed. Although standard radical gastrectomy and postoperative chemotherapy can benefit GC patients to some extent, the prognosis of most patients is still poor (Liu *et al.*, 2021; Sun *et al.*, 2021a). Thus, it is important to find novel effective drugs that can serve as adjuvant therapy for GC and to explore new therapeutic targets for GC in order to improve the survival rate, prognosis, and quality of life of patients with this disease (Liu and Henkel, 2002; Sun *et al.*, 2021b).

Traditional Chinese medicine (TCM) has long been used to treat clinical diseases and has made great contributions to improving the health of people worldwide (Xu and Zhang, 2020). The extraction of effective substances from TCM has become an important means to obtain compounds with low toxicity and anti-tumor effects for the treatment of advanced cancer. In the past several decades, great advancements have been made in the utilization of Schisandrin B (Sch B), which is extracted from the TCM *Schisandra chinensis* (Turcz) Baillon, for the prevention and treatment of cancer, confirming the potential application of TCM as a treatment strategy for cancer (Zhong *et al.*, 2021). Sch B has been shown to have strong inhibitory effects on liver cancer cells (Wu *et al.*, 2004) and strong toxicity in colon cancer cells (Li *et al.*, 2019). Sch B can also inhibit the viability of lung cancer cells by activating the nuclear factor kappa B (NF-κB) and mitogen-activated protein kinase (MAPK) signaling pathways (Li *et al.*, 2021). In addition, Sch B may be the only compound that has been confirmed to have great potential

*Address correspondence to: Yinghua Luo, luoyinghua202208@163.com; Chenghao Jin, jinchenghao3727@byau.edu.cn
#These authors contributed equally to this work
Received: 21 July 2022; Accepted: 17 August 2022

Doi: 10.32604/biocell.2023.025593 www.techscience.com/journal/biocell

This work is licensed under a Creative Commons Attribution 4.0 International License, which permits unrestricted use, distribution, and reproduction in any medium, provided the original work is properly cited.

for anti-cancer application, as it can be used as both a chemotherapeutic sensitizer and a myocardial protective agent (Xu *et al.*, 2011). Previous studies have also shown that Sch B induces cell cycle arrest and triggers cell apoptosis by inhibiting signal transducer and activator of transcription 3 (STAT3) phosphorylation and nuclear translocation, thus exhibiting effective anticancer activity against triple-negative breast cancer (Dai *et al.*, 2018). Interestingly, studies have found that Sch B can promote the accumulation of ROS in hepatocellular carcinoma HEPA1-6 cells, then induce ROS-mediated autophagy and Th1/Th2 imbalance, and finally play an anticancer role (Tan *et al.*, 2022). Although it is known that Sch B can affect the MAPK, STAT3, and NF-κB signaling pathways, in-depth information is still lacking.

Therefore, we focused on Sch B as a research target to explore whether Sch B can affect reactive oxygen species (ROS) levels in GC cells to induce apoptosis, cell cycle arrest, and inhibition of cell migration through the MAPK, STAT3, and NF-κB pathways.

Materials and Methods

Cell lines and cell culture

GC cells (AGS, KATO-3, MKN-28, MKN-45, NCI-N87, SNU-5, SNU-216, SNU-484, SNU-668, YCC-1, YCC-6, and YCC-16) and normal cells were purchased from Otwo Biotech Inc. (ShenZhen, China), BeNa Culture Collection (Henan, China), and Bluef Biotechnology Development Co., Ltd. (Shanghai, China). The cells were cultured with RPMI 1640 and DMEM medium (Gibco, Waltham, USA) supplemented with 10% FBS (Gibco), 100 U/mL penicillin (Gibco), and 100 μg/mL streptomycin (Gibco).

Cell counting kit-8 assay

Cells were cultured in 96-well plates at 5% CO_2 in a 37°C incubator (Sanyo, Osaka, Japan), and treated with different concentrations of Sch B (Herbpurify, Chengdu, China) and Cisplatin (DDP) (Solarbio Life Science, Beijing, China) for 24 h. The effects of Sch B on cell viability were determined using the Cell Counting Kit-8 (Solarbio), and cell viability was determined using enzyme-linked immunosorbent assay (Tecan Inc., Switzerland).

Analysis of cell apoptosis

Apoptosis morphology was detected by the Hoechst 33342/propidium iodide (PI) double staining Kit (Solarbio) and visualized using the EVOS FL automated cell imaging system (Thermo Fisher Scientific, USA). The number of apoptotic cells and mitochondrial membrane potential were detected using the Annexin V Apoptosis Detection Kit (Solarbio) and Mitochondrial Membrane Potential Detection Kit (Solarbio) according to the manufacturer's instructions. The cell cycle was analyzed by flow cytometry (Beckman Coulter, Inc., USA).

Measurement of cellular ROS levels

Intracellular ROS levels in GC AGS cells were measured using the Reactive Oxygen Species Assay Kit (Beyotime, China) according to the manufacturer's instructions. At 30 min before Sch B treatment, AGS cells were pretreated with 10 μM N-acetylcysteine (NAC) (Beyotime) and the number of apoptotic cells was detected by flow cytometry.

Cell cycle analysis

The DNA Content Quantitation Assay (Solarbio) was used to detect the number of cells in different cell cycles according to the manufacturer's instructions. The cell cycle was detected by flow cytometry.

Wound healing assay

When AGS cells were cultured to exponentially increase, "wounds" were introduced by scratching the cells with a 200 μL pipette tip, and the culture medium containing Sch B was replaced to treat the cells. The changes in the cells at different time points were observed under an inverted microscope (Mshot, China).

Western blot analysis

Proteins were resolved on a 10–12% SDS-PAGE gel, electrotransferred to nitrocellulose membranes (Pall Co., Hauppauge, USA), and blocked in 5% skim milk (Becton Dickinson, NJ, USA). Then membranes were incubated overnight at 4°C with primary antibody (Santa Cruz Biotechnology, Inc., Dallas, USA), and then incubated for 2–4 h with goat anti-mouse IgG or goat anti-rabbit IgG secondary antibody (ZSGB Bio, Inc., Beijing, China). Proteins were detected by enhanced chemiluminescence (Pierce, Thermo Fisher Scientific), and the Amersham Imager 600 (GE, Fairfield, USA) was used to capture the chemiluminescence images. For inhibitor-treated cell samples, at 30 min before Sch B treatment, AGS cells were pretreated with 10 μM MAPK inhibitors (p38 inhibitor, SB203580; JNK inhibitor SP600125; ERK inhibitor FR180204) (MedChem Express, USA), and then the protein was detected.

Statistical analyses

The bar charts were made using Excel software and analyzed by SPSS 22.0. The results are expressed as the mean ± standard deviation, and the differences between groups were analyzed by the *t*-test. $P < 0.05$ was considered statistically significant.

Results

IC_{50} of Sch B in human GC cells lines

As shown in Fig. 1A, 12 kinds of GC cells were treated with different concentrations of DDP and Sch B for 24 h. Sch B showed excellent inhibition of the cell viability of 12 kinds of GC cells, with an IC_{50} of 53.7 μM for the most sensitive AGS cells, which was significantly stronger than the effect of the DDP group (Table 1). However, compared with DDP, cell viability was not significantly inhibited in the four normal cells after Sch B treatment (Fig. 1B).

Sch B induces apoptosis in AGS cells

Taking the gastric cancer AGS cells that were most sensitive to Sch B as an example, compared with the 0 h control, the apoptotic fluorescence intensity of AGS cells treated with Sch B for 24 h was significantly enhanced, and the apoptotic number of AGS cells was significantly increased (Figs. 2A and 2B). The mitochondrial membrane potential red/green

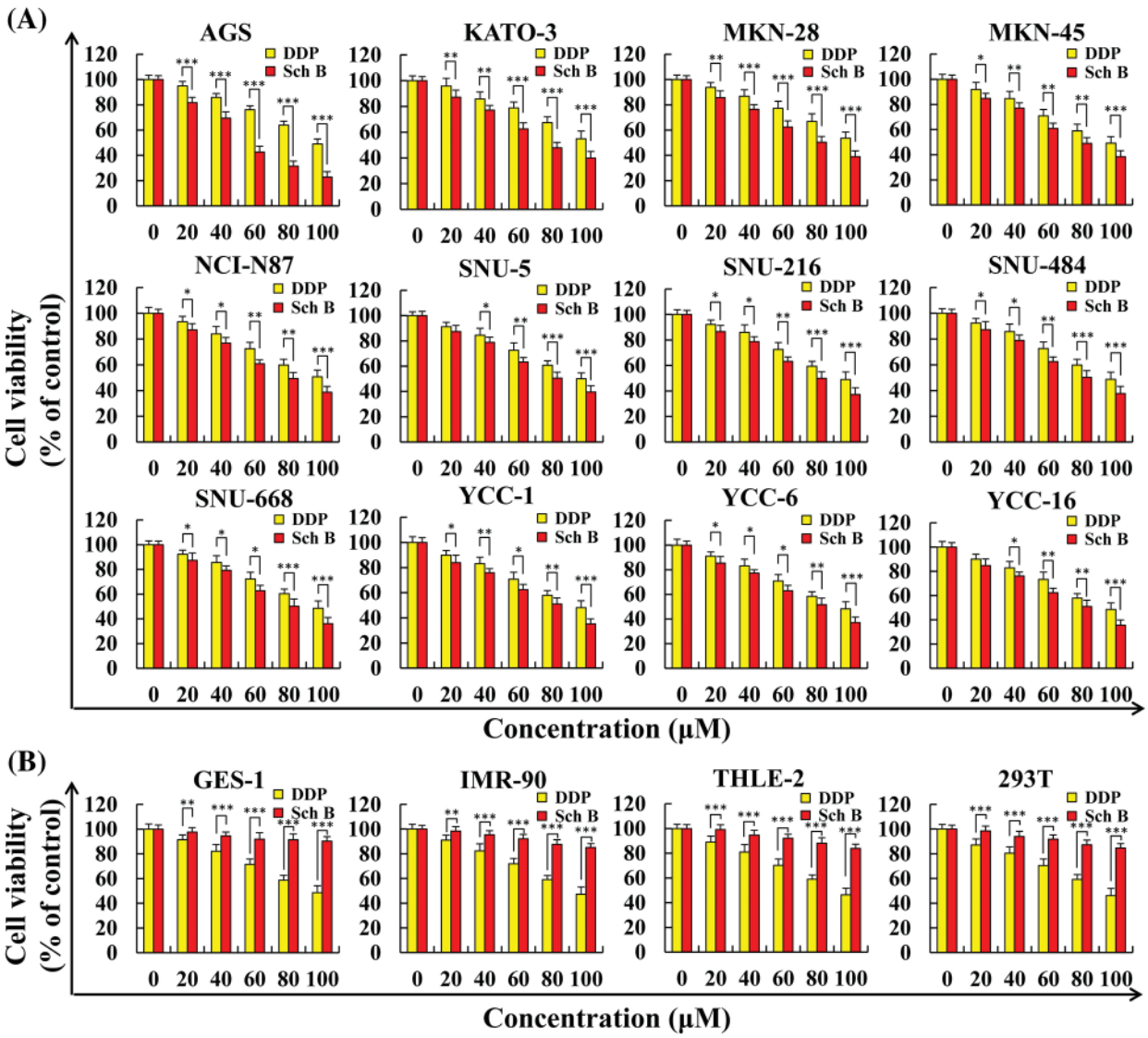

FIGURE 1. Sch B inhibited the proliferation of GC cells but did not affect the growth of normal cells. (A) The proliferation curve of GC cells after Sch B and DDP treatment. (B) The proliferation curve of normal cells after Sch B and DDP treatment. Representative data from at least three independent experiments. *, $P < 0.05$; **, $P < 0.01$; ***, $P < 0.001$.

TABLE 1

Concentrations IC_{50} value of DDP and Sch B in Twelve GC cell lines

Number	Cell name	DDP (μM)	Sch B (μM)
1	AGS	99.83 ± 1.42	53.74 ± 1.42
2	KATO-3	>100	74.14 ± 1.31
3	MKN-28	>100	80.23 ± 1.11
4	MKN-45	98.79 ± 1.83	80.40 ± 1.52
5	NCI-N87	>100	79.43 ± 1.38
6	SNU-5	96.38 ± 1.24	78.34 ± 2.04
7	SNU-216	95.35 ± 1.52	79.34 ± 1.24
8	SNU-484	95.42 ± 2.01	78.24 ± 1.63
9	SNU-668	99.82 ± 1.16	82.33 ± 1.64
10	YCC-1	99.35 ± 1.27	83.65 ± 1.56
11	YCC-6	98.45 ± 1.86	84.64 ± 2.01
12	YCC-16	95.53 ± 1.74	80.84 ± 1.76

fluorescence ratio ranged from 2.85 to 0.99, i.e., the level of mitochondrial membrane potential decreased continuously (Fig. 2C). After Sch B treatment for 24 h, the expression levels of the pro-apoptotic proteins Bad, cleaved(cle)-caspase-3, cleaved(cle)-PARP, and cytochrome C significantly increased. The expression levels of the anti-apoptotic proteins Bcl-2 and pro-caspase-3 significantly reduced (Fig. 2D). It was thus proven that Sch B induced apoptosis of gastric cancer AGS cells by damaging mitochondria.

Sch B effects on the MAPK/STAT3/NF-κB signaling pathways in AGS cells

After treatment with Sch B for 24 h, the expression levels of p-ERK, p-STAT3, and NF-κB significantly decreased. Compared with the control group, Sch B significantly increased the expression levels of p-JNK and p-p38 in AGS cells (Fig. 3A). After pretreatment with FR180204 (ERK inhibitor), SB203580 (P38 inhibitor), and SP600125 (JNK inhibitor), the expression of p-ERK significantly increased, while the expression of p-p38 and p-JNK significantly

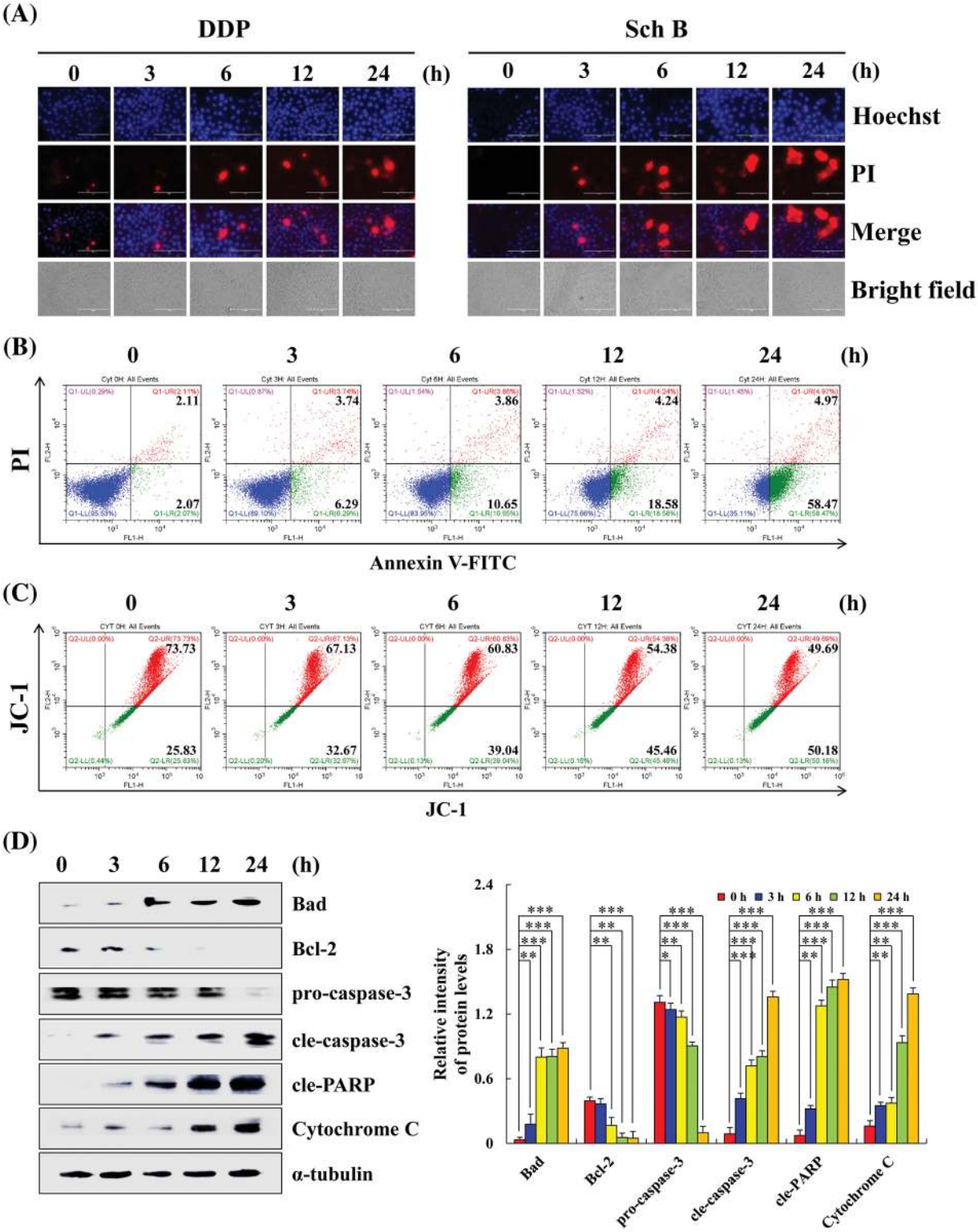

FIGURE 2. Sch B induces AGS cells apoptosis in a concentration-dependent manner. (A) Hoechst 33342/PI (blue and red fluorescence) was used to observe the apoptotic morphology of AGS cells (magnification: 400×). (B) Annexin V-FITC/PI (green and red fluorescence) was used to determine the number of early and late apoptotic cells by flow cytometry. (C) JC-1 was analyzed to determine the mitochondrial membrane potential by flow cytometry. (D) Sch B promoted the apoptosis of AGS cells in GC was detected by Western blotting. Representative images from at least three independent experiments. *, $P < 0.05$; **, $P < 0.01$; ***, $P < 0.001$.

decreased. In addition, the expression of p-STAT3 and cle-caspase-3 increased and decreased in the Sch B+ERK/p38/JNK inhibitor group compared with the Sch B alone treatment group. However, the expression of cle-caspase-3 in the Sch B +p38 inhibitor group increased (Figs. 3B–3D).

Sch B affects ROS levels and MAPK/STAT3/NF-κB expression in human AGS cells

After treatment with Sch B for 24 h, the percent of ROS accumulation in AGS cells ranged from 39.25% to 67.81% (considered the middle of the abscissa of the experimental results

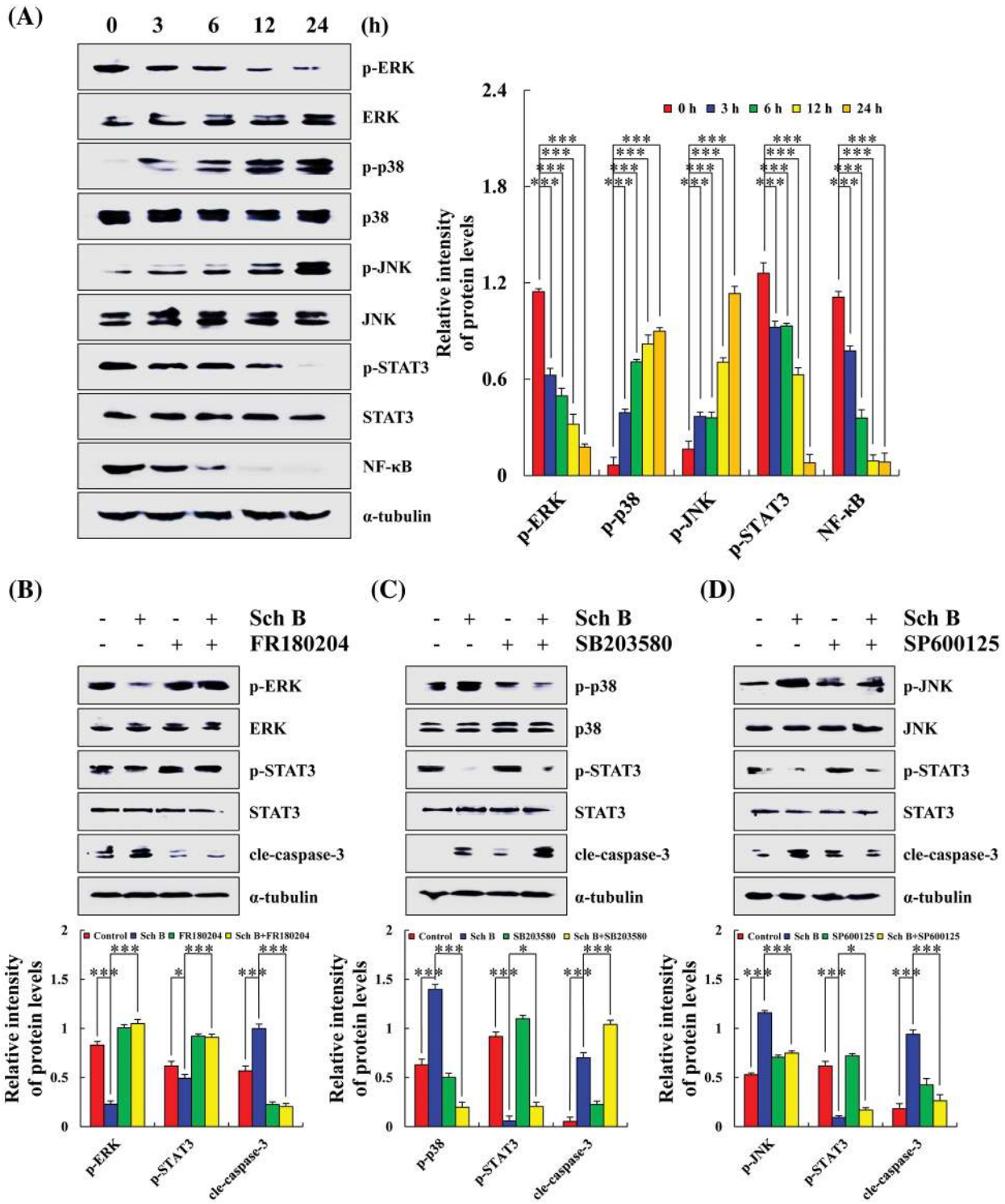

FIGURE 3. Sch B affected the expression of MAPK/STAT3/NF-κB pathway proteins and induced the early apoptosis of AGS cells. (A) Western blotting of ERK, p38, JNK, STAT3, NF-κB, with α-tubulin as the internal control. (B–D) Detection of the effects of Sch B on MAPK and STAT3 protein expression after pretreatment of AGS cells with FR180204/SB203580/SP600125. Representative data from at least three independent experiments. *, $P < 0.05$; **, $P < 0.01$; ***, $P < 0.001$.

as the boundary, and set different colors to make the experimental results more intuitive), while the percentage of cells that underwent apoptosis in the Sch B group was 27.89%. The percent of apoptotic cells in the Sch B+NAC group was 8.74% (Figs. 4A and 4B). Higher p-ERK, p-STAT3, and NF-κB expression in the Sch B+NAC groups was detected compared with that in the Sch B group in AGS cells, while lower p-p38, p-JNK, cle-caspase-3, and cle-PARP expression levels were detected (Fig. 4C).

Sch B arrest AGS cell cycle in G0/G1

After treatment with Sch B for 24 h, the number of AGS cells in the G0/G1 phase increased by 59.65% and that in the G2/M phase decreased by 22.18% compared with the control group at 0 h (Fig. 5A). Higher p21 and p27 expression was observed, whereas lower CDK2, CDK4, CDK6, cyclin D1, and cyclin E expression levels in the 24 h Sch B group compared with the 0 h group in AGS cells were found (Fig. 5B).

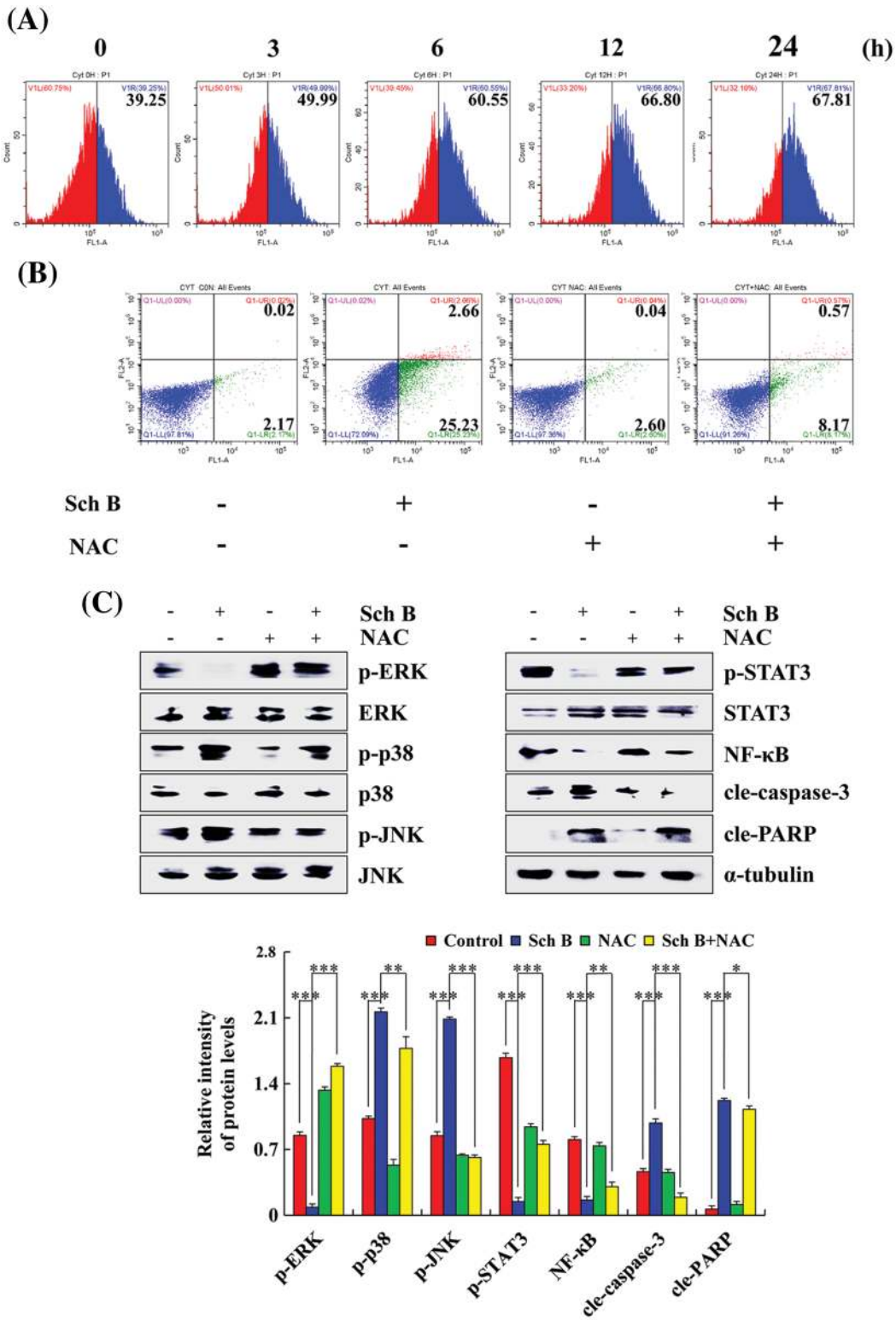

FIGURE 4. Effects of Sch B on AGS cell apoptosis after an increase in ROS level. (A) DCFH-DA was analyzed to determine the ROS content by flow cytometry. (B) Annexin V-FITC/PI was used to determine the number of early and late apoptotic cells by flow cytometry after NAC pretreatment. (C) The effects of Sch B on the proteins of mediated signaling pathways in GC cells were detected by Western blotting after NAC pretreatment, with α-tubulin as the internal control. Representative data from at least three independent experiments. *, $P < 0.05$; **, $P < 0.01$; ***, $P < 0.001$.

Sch B inhibits AGS cell migration, in which ROS plays an important role

After treatment with Sch B for 24 h, the migration area of AGS cells was inhibited compared with the control at 0 h (Fig. 6A). The expression levels of β-catenin and SNAI1 (cancer metastasis inducible factor) in AGS cells in the 24 h Sch B group decreased, and the expression level of E-cadherin increased (Fig. 6C). After NAC treatment, cell migration area and related migration protein levels were significantly reversed (Figs. 6B and 6D).

Discussion

One of the biggest challenges for researchers is treating cancer (Zaromytidou, 2021). Traditional treatment options such as

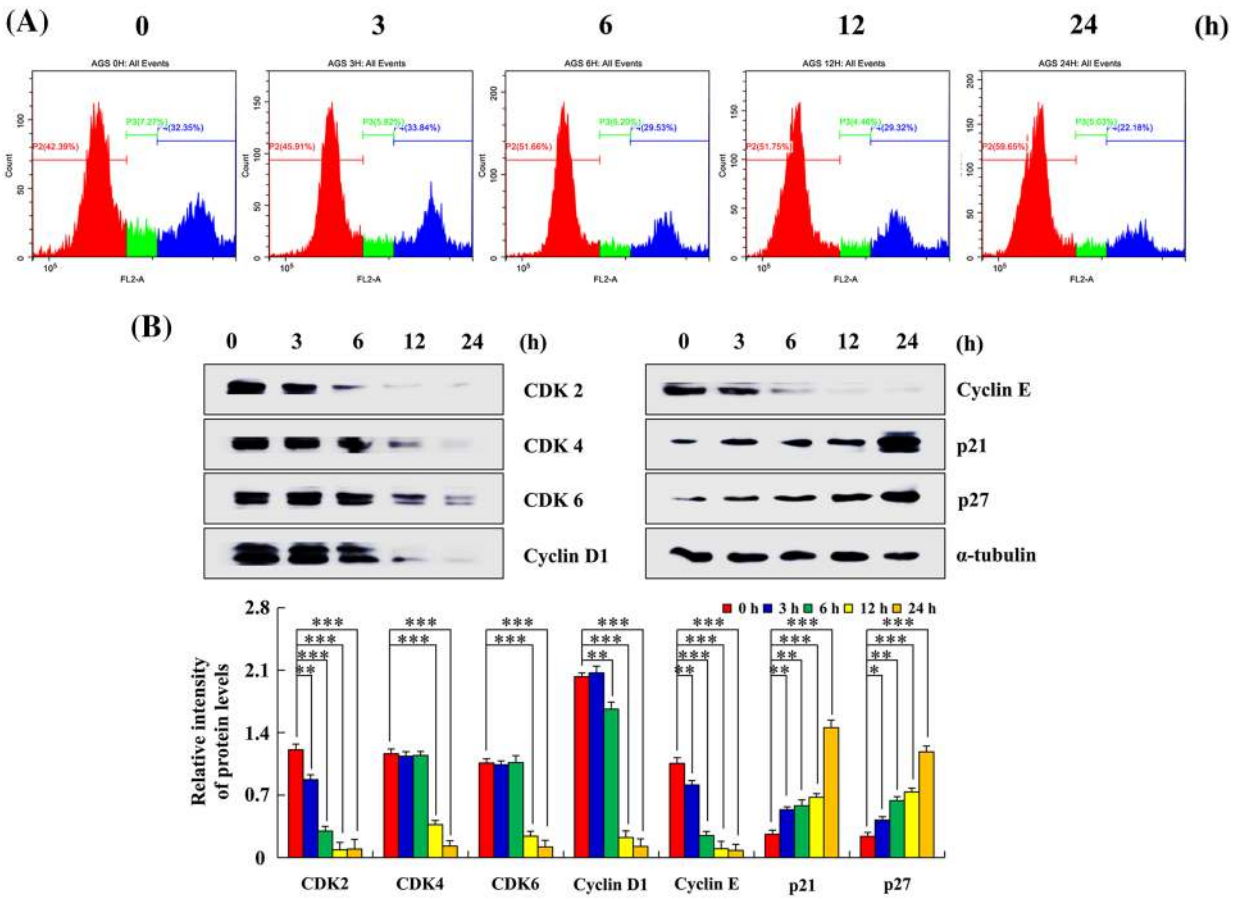

FIGURE 5. Effects of Sch B on the cell cycle and cycle-related protein expression. (A) PI was analyzed to determine the DNA content by flow cytometry. (B) Sch B effects on CDK2/4/6, cyclin D1/E, and p21/27 expression were detected by Western blotting, with α-tubulin as the internal control. Representative data from at least three independent experiments. *, $P < 0.05$; **, $P < 0.01$; ***, $P < 0.001$.

chemotherapy, radiation, surgery, and combination therapy have been widely accepted to treat cancer. While chemotherapy remains an effective cancer treatment, it is overwhelmingly associated with severe side effects, and cancers can evolve to resist chemotherapy and radiation (Baskar *et al.*, 2012). Therefore, finding new therapeutic methods is necessary to accurately treat tumors and prevent tumor metastasis (Zhang *et al.*, 2021). Therefore, to overcome the major obstacles of traditional cancer treatment, researchers are looking for effective treatments such as alternative and complementary therapies (Yaghoubi *et al.*, 2022).

Sch B is a lignan extracted from Schisandrae. Sch B can inhibit the proliferation and invasion of human lung adenocarcinoma A549 cells and glioma cells (Zhuang *et al.*, 2019). It can effectively reduce the activation of inflammatory signaling pathways including the NF-κB and MAPK (ERK/p38/JNK) pathways (Ran *et al.*, 2018). Many studies have verified that Sch B has protective effects on inflammatory bowel disease and acute lung injury. The MTT assay was used to detect the toxicity of Sch B in HCCLM3 hepatocellular carcinoma cells. The results showed that low concentrations (<20 μmol/L) had no significant effects on the viability of HCCLM3 cells. A high concentration (>20 μmol/L) of Sch B significantly reduced cell viability (Chen *et al.*, 2021). However, Sch B has a variety of potential cell-protective activities against normal renal proximal convoluted tubule HK-2 cells (Liu *et al.*, 2018). Similarly, in our study, a high concentration of Sch B had good inhibitory effects on GC cell proliferation, and the inhibitory effect was significantly better than that of the DDP group. In addition, Sch B had no significant toxic effects on normal cells (Fig. 1).

Sch B showed strong anti-tumor activity by inducing cholangiocarcinoma (CCA) apoptosis, which may be a promising drug for treating CCA. Annexin V/PI double staining showed that Sch B induced apoptosis of intrahepatic CCA cells. Rhodamine 123 staining showed a dose-dependent decrease of mitochondrial membrane potential with Sch B treatment (Yang *et al.*, 2016). In addition, Sch B induces apoptosis by upregulating B-cell lymphoma 2-associated X protein, cleaved caspase-3/9, cleaved PARP, and downregulating Bcl-2, cyclin D1, and CDK4 (Lv *et al.*, 2015). Sch B significantly inhibited the growth of xenograft tumor HCCC-9810 in nude mice (Yang *et al.*, 2016). In this study, we also observed that the number of AGS cells apoptosis significantly increased and obvious apoptotic morphology appeared after Sch B treatment. The level of apoptotic proteins also changed at the molecular level. The above experiments indicated that Sch B could induce the apoptosis of AGS cells, and its molecular mechanism was similar to that described in previous works (Fig. 2).

The various biochemical pathways comprise a series of different proteins that exert different physiological and biochemical functions; when apoptosis occurs, the pathway relays signals (Deel *et al.*, 2015). Sch B has certain effects on

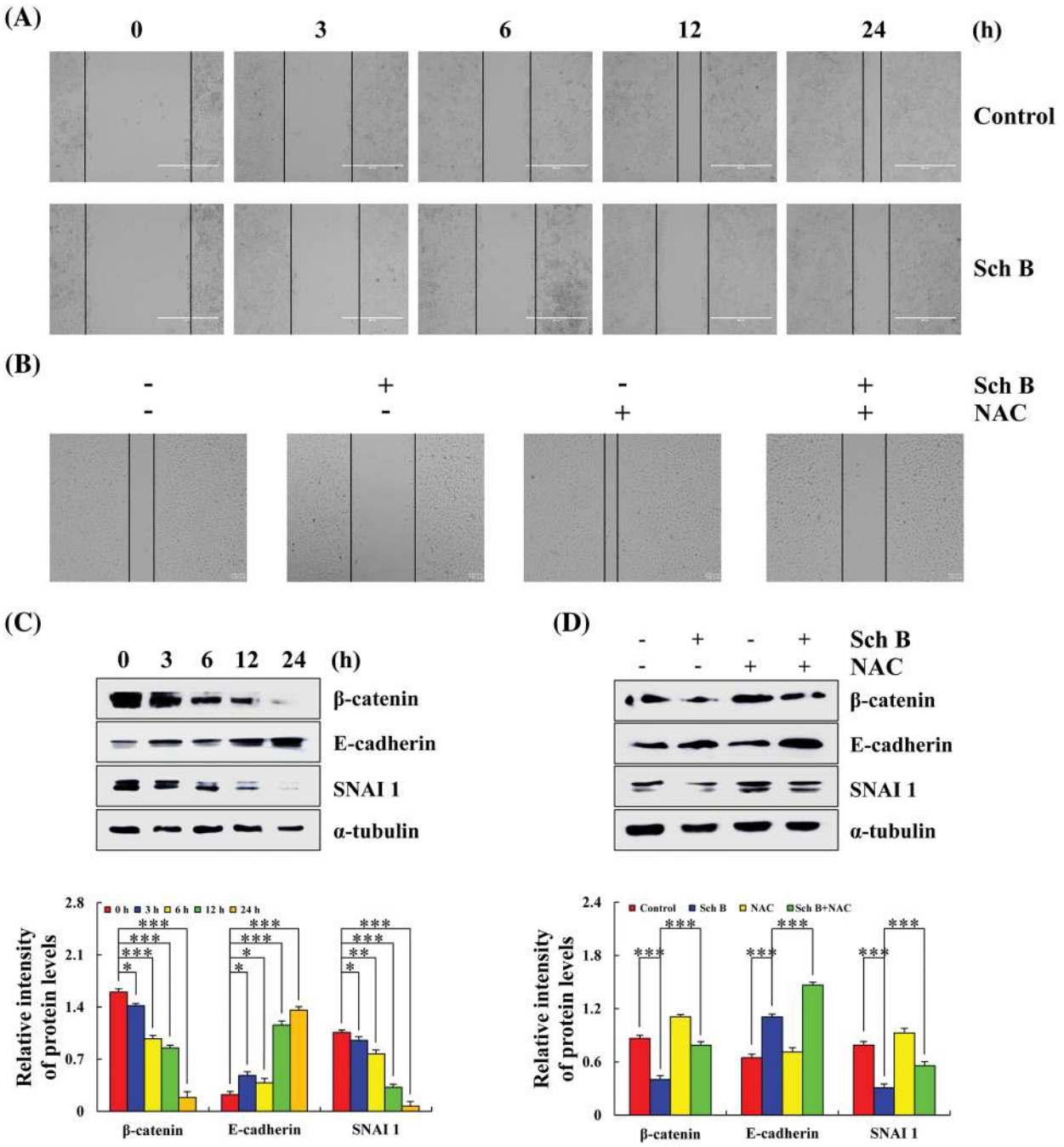

FIGURE 6. Effects of Sch B on cell migration and the expression of E-cadherin, SNAI1, and β-catenin migration proteins. (A) The phenomenon of migrating cells was observed by a cell scratch experiment. (magnification: 400×) (B) The migration of AGS cells was observed after adding the scavenger NAC. (magnification: 400×) (C) The migration protein of Sch B mediated E-cadherin, SNAI1, and β-catenin. (D) After NAC pretreatment, the migration proteins were detected by Western blotting, with α-tubulin as the internal control. Representative data from at least three independent experiments. *, $P < 0.05$; **, $P < 0.01$; ***, $P < 0.001$.

the activation of three members of the MAPK family during SiO1-induced lung tissue injury, and the intervention of Sch B at the initial stage of silicon infection can inhibit the activation of NF-κB (Li *et al.*, 2010). In addition, Sch B has protective effects on the oxidative stress injury of H9c2 cells by activating the JAK2/STAT3 signaling pathway (Wang and Huang, 2020). Similarly, our study showed that Sch B could regulate the expression levels of the ERK, p38, JNK, STAT3, and NF-κB pathways. In addition, the addition of ERK (FR180204), p38 (SB203580), and JNK (SP600125) inhibitors suggests that ERK/p38/JNK is upstream of the STAT3 pathway. These results suggest that Sch B may promote AGS cell apoptosis by regulating the MAPK/STAT3/NF-κB signaling pathways (Fig. 3).

Tumor cells have higher ROS levels and are more sensitive to ROS, leading to a state of oxidative stress in tumor cells (Benhar *et al.*, 2002). In recent years, continuous exploration and research on ROS have found that higher ROS content can accelerate the death of tumor cells, which provides a clinical basis for the treatment of cancer with gemcitabine and arsenic trioxide, and other pro-oxidation chemotherapy drugs (Jia *et al.*, 2020). Previous studies have

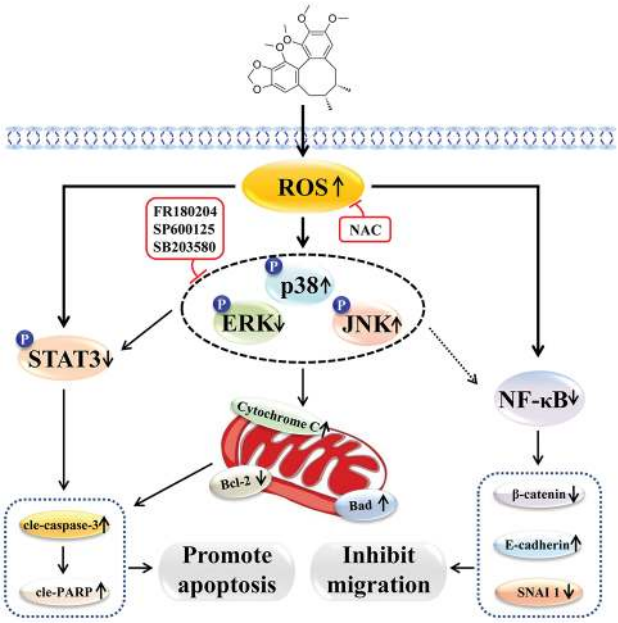

FIGURE 7. Schematic diagram of the molecular mechanism of Sch B-induced apoptosis, migration, and cycle of GC cells.

suggested that Sch B may induce the apoptosis of MDA-MB-231 cells by increasing ROS and stimulating the expression of endoplasmic reticulum stress-related proteins CCAAT-enhancer-binding protein homologous protein, G protein-coupled receptor 78, and p-eukaryotic initiation factor 2 alpha (Dai *et al.*, 2018). In this study, Sch B increased ROS levels with increasing doses. After adding NAC, the number of apoptotic AGS cells was significantly lower than that in the Sch B alone group. In addition, NAC also decreased the Sch B-mediated increase in MAPK/STAT3/NF-κB protein expression. The results showed that Sch B could accumulate the ROS-mediated MAPK/STAT3/NF-κB signaling pathway and promote mitochondria-dependent apoptosis (Fig. 4).

The precise control of the cell cycle has a major influence on the differentiation, development, heredity, and survival activities of the organism. Dysregulation of the cell cycle is a hallmark of tumor cells. Previous studies have shown that Sch B can inhibit the proliferation and abnormal mitosis of human gastric cancer SCG-7901 cells, which may be caused by the downregulation of cyclin D1 mRNA expression (Liu *et al.*, 2007). In this study, we used flow cytometry and Western blotting to show that that Sch B arrested the AGS cell cycle in the G0/G1 phase (Fig. 5). In various cancer types, the epithelial-mesenchymal transformation is a necessary step for tumor metastasis (Ribatti *et al.*, 2020). The mechanism of existing anti-tumor metastasis drugs is mostly to kill tumor cells, which also causes harm to normal cells and causes painful side effects (Fontebasso and Dubinett, 2015). *In vivo* studies have shown that surgical treatment of early, middle, and advanced breast cancer combined with Sch B can reduce the number of breast cancer metastases and prolong the survival time of breast cancer-bearing mice (Liu *et al.*, 2012). In this study, Sch B inhibited the migration of AGS cells. Moreover, the active oxygen scavenger NAC blocked Sch B-mediation inhibition of cell migration. The results showed that Sch B upregulated ROS and inhibited cell migration (Fig. 6).

Conclusion

In conclusion, Sch B has good killing effects on GC cells, possibly by upregulating intracellular ROS, activating the MAPK/STAT3/NF-κB signaling pathway, arresting the cell cycle, inhibiting cell migration, and inducing mitochondria-dependent apoptosis (Fig. 7).

Acknowledgement: We thank LetPub (www.letpub.com) for its linguistic assistance during the preparation of this manuscript.

Availability of Data and Materials: The datasets generated during and/or analysed during the current study are available from the corresponding author on reasonable request.

Author Contribution: The authors confirm contribution to the paper as follows: study conception and design: Tian-Zhu Li, Yu Zhang and Tong Zhang; data collection: Yan-Nan Li and Hui Xue; analysis and interpretation of results: Jing-Long Cao and Wen-Shuang Hou; draft manuscript preparation: Ying-Hua Luo and Cheng-Hao Jin. All authors reviewed the results and approved the final version of the manuscript.

Ethics Approval: Not applicable.

Funding Statement: This work was supported by the National Natural Science Foundation of China [Grant No. 82060118]; the Research Program of Science and Technology at Universities of Inner Mongolia Autonomous Region [Grant No. NJZY20203]; the Program for Young Talents of Chifeng University [Grant No. CFXYYT2202]; the Central Government Supports Local College Reform and Development Fund Talent Training Projects [Grant No. 2020GSP16]; the Heilongjiang Touyan Innovation Team Program [Grant No. 2019HTY078]; and the Project for Heilongjiang Bayi Agricultural University [Grant No. XDB202012].

Conflicts of Interest: The authors declare that they have no conflicts of interest to report regarding the present study.

References

Baskar R, Lee KA, Yeo R, Yeoh KW (2012). Cancer and radiation therapy: Current advances and future directions. *International Journal of Medical Sciences* **9**: 193–199. DOI 10.7150/ijms.3635.

Benhar M, Engelberg D, Levitzki A (2002). ROS, stress-activated kinases and stress signaling in cancer. *EMBO Reports* **3**: 420–425. DOI 10.1093/embo-reports/kvf094.

Chen Q, Bao L, Lv L, Xie F, Zhou X, Zhang H, Zhang G (2021). Schisandrin B regulates macrophage polarization and alleviates liver fibrosis via activation of PPARγ. *Annals of Translational Medicine* **9**: 1500. DOI 10.21037/atm-21-4602.

Dai X, Yin C, Guo G, Zhang Y, Zhao C, Qian J, Wang O, Zhang X, Liang G (2018). Schisandrin B exhibits potent anticancer activity in triple negative breast cancer by inhibiting STAT3. *Toxicology and Applied Pharmacology* **358**: 110–119. DOI 10.1016/j.taap.2018.09.005.

Deel MD, Li JJ, Crose LE, Linardic CM (2015). A review: Molecular aberrations within hippo signaling in bone and soft-tissue sarcomas. *Frontiers in Oncology* **5**: 190. DOI 10.3389/fonc.2015.00190.

Fontebasso Y, Dubinett SM (2015). Drug development for metastasis prevention. *Critical Reviews in Oncogenesis* **20**: 449–473. DOI 10.1615/CritRevOncog.v20.i5-6.150.

Jia P, Dai C, Cao P, Sun D, Ouyang R, Miao Y (2020). The role of reactive oxygen species in tumor treatment. *RSC Advances* **10**: 7740–7750. DOI 10.1039/C9RA10539E.

Li SF, Liu TF, Guo M, Wang ZP, Fan LH (2010). Effect of Schisandrin B on mitogen-activated protein kinases and nuclear factor-kappaB in rat lungs exposed to silica. *Chinese Journal of Industrial Hygiene and Occupational Diseases* **28**: 329–333.

Li J, Lu Y, Wang D, Quan F, Chen X et al. (2019). Schisandrin B prevents ulcerative colitis and colitis-associated-cancer by activating focal adhesion kinase and influence on gut microbiota in an *in vivo* and *in vitro* model. *European Journal of Pharmacology* **854**: 9–21. DOI 10.1016/j.ejphar.2019.03.059.

Li S, Wang H, Ma R, Wang L (2021). Schisandrin B inhibits epithelial-mesenchymal transition and stemness of large-cell lung cancer cells and tumorigenesis in xenografts via inhibiting the NF-κB and p38 MAPK signaling pathways. *Oncology Reports* **45**: 115. DOI 10.3892/or.2021.8066.

Liu J, Henkel T (2002). Traditional Chinese Medicine (TCM): Are polyphenols and saponins the key ingredients triggering biological activities. *Current Medicinal Chemistry* **9**: 1483–1485. DOI 10.2174/0929867023369709.

Liu Q, Song J, Li H, Dong L, Dai S (2018). Schizandrin B inhibits the cis DDP induced apoptosis of HK 2 cells by activating ERK/NF κB signaling to regulate the expression of surviving. *International Journal of Molecular and Cellular Medicine* **41**: 2108–2116. DOI 10.3892/ijmm.2018.3409.

Liu SJ, Yang YB, Zhou JX, Lin YJ, Pan YL, Pan JH (2021). A novel ferroptosis-related gene risk signature for predicting prognosis and immunotherapy response in gastric cancer. *Disease Markers* **2021**: 2385406. DOI 10.1155/2021/2385406.

Liu XN, Zhang CY, Jin XD, Li YZ, Zheng XZ, Li L (2007). Inhibitory effect of schisandrin B on gastric cancer cells *in vitro*. *World Journal of Gastroenterology* **13**: 6506–6511. DOI 10.3748/wjg.v13.i48.6506.

Liu Z, Zhang B, Liu K, Ding Z, Hu X (2012). Schisandrin B attenuates cancer invasion and metastasis via inhibiting epithelial-mesenchymal transition. *PLoS One* **7**: e40480. DOI 10.1371/journal.pone.0040480.

Lv XJ, Zhao LJ, Hao YQ, Su ZZ, Li JY, Du YW, Zhang J (2015). Schisandrin B inhibits the proliferation of human lung adenocarcinoma A549 cells by inducing cycle arrest and apoptosis. *International Journal of Clinical and Experimental Medicine* **8**: 6926–6936.

Ran J, Ma C, Xu K, Xu L, He Y et al. (2018). Schisandrin B ameliorated chondrocytes inflammation and osteoarthritis via suppression of NF-κB and MAPK signal pathways. *Drug Design Development and Therapy* **12**: 1195–1204. DOI 10.2147/DDDT.

Rawla P, Barsouk A (2019). Epidemiology of gastric cancer: Global trends, risk factors and prevention. *Przeglad Gastroenterologiczny* **14**: 26–38. DOI 10.5114/pg.2018.80001.

Ribatti D, Tamma R, Annese T (2020). Epithelial-mesenchymal transition in cancer: A historical overview. *Translational Oncology* **13**: 100773. DOI 10.1016/j.tranon.2020.100773.

Sun Y, Jin J, Jing H, Lu Y, Zhu Q, Shu C, Zhang Q, Jing D (2021a). ITIH4 is a novel serum biomarker for early gastric cancer diagnosis. *Clinica Chimica Acta* **523**: 365–373. DOI 10.1016/j.cca.2021.10.022.

Sun KR, Lv HF, Chen BB, Nie CY, Zhao J, Chen XB (2021b). Latest therapeutic target for gastric cancer: Anthrax toxin receptor 1. *World Journal of Gastrointestinal Oncology* **13**: 216–222. DOI 10.4251/wjgo.v13.i4.216.

Tan S, Zheng Z, Liu T, Yao X, Yu M, Ji Y (2022). Schisandrin B induced ROS-mediated autophagy and Th1/Th2 imbalance via selenoproteins in Hepa1-6 cells. *Frontiers in Immunology* **13**: 857069. DOI 10.3389/fimmu.2022.857069.

Wang L, Huang J (2020). Schisandrin B regulating Jak2/Stat3 signaling pathway in the inhibitionof oxidative stress damage of myocardial cells. *Western Journal of Traditional Chinese Medicine* **33**: 11–13. DOI 10.12174/j.issn.1004-6852.2020.02.03.

Wu YF, Cao MF, Gao YP, Chen F, Wang T, Zumbika EP, Qian KX (2004). Down-modulation of heat shock protein 70 and up-modulation of Caspase-3 during schisandrin B-induced apoptosis in human hepatoma SMMC-7721 cells. *World Journal of Gastroenterology* **10**: 2944–2948. DOI 10.3748/wjg.v10.i20.2944.

Xu Y, Liu Z, Sun J, Pan Q, Sun F, Yan Z, Hu X (2011). Schisandrin B prevents doxorubicin-induced chronic cardiotoxicity and enhances its anticancer activity *in vivo*. *PLoS One* **6**: e28335. DOI 10.1371/journal.pone.0028335.

Xu J, Zhang Y (2020). Traditional Chinese Medicine treatment of COVID-19. *Complementary Therapies in Clinical Practice* **39**: 101165. DOI 10.1016/j.ctcp.2020.101165.

Yaghoubi F, Motlagh NSH, Naghib SM, Haghiralsadat F, Jaliani HZ, Moradi A (2022). A functionalized graphene oxide with improved cytocompatibility for stimuli-responsive co-delivery of curcumin and doxorubicin in cancer treatment. *Scientific Reports* **12**: 1959. DOI 10.1038/s41598-022-05793-9.

Yang X, Wang S, Mu Y, Zheng Y (2016). Schisandrin B inhibits cell proliferation and induces apoptosis in human cholangiocarcinoma cells. *Oncology Reports* **36**: 1799–1806. DOI 10.3892/or.2016.4992.

Zaromytidou AI (2021). Cancer research that matters. *Nature Cancer* **2**: 1268–1270. DOI 10.1038/s43018-021-00302-9.

Zhang Z, Lu M, Qin Y, Gao W, Tao L, Su W, Zhong J (2021). Neoantigen: A new breakthrough in tumor immunotherapy. *Frontiers in Immunology* **12**: 672356. DOI 10.3389/fimmu.2021.672356.

Zhong L, Li Y, Xiong L, Wang W, Wu M et al. (2021). Small molecules in targeted cancer therapy: Advances, challenges, and future perspectives. *Signal Transduction and Targeted Therapy* **6**: 201. DOI 10.1038/s41392-021-00572-w.

Zhuang W, Li Z, Dong X, Zhao N, Liu Y, Wang C, Chen J (2019). Schisandrin B inhibits TGF-β1-induced epithelial-mesenchymal transition in human A549 cells through epigenetic silencing of ZEB1. *Experimental Lung Research* **45**: 157–166. DOI 10.1080/01902148.2019.1631906.